



ELSEVIER

Available online at www.sciencedirect.com

SCIENCE @ DIRECT®

Journal of Magnetism and Magnetic Materials 286 (2005) 146–149



www.elsevier.com/locate/jmmm

Barrier characteristic in Nb/Ni planar tunnel junctions

E.M. González^{a,*}, F.J. Palomares^b, R. Escudero^a, J.E. Villegas^a,
J.M. González^b, J.L. Vicent^a

^a*Departamento de Física de Materiales, Facultad de CC. Físicas, Universidad Complutense, 28040 Madrid, Spain*

^b*Instituto de Ciencia de Materiales de Madrid, CSIC, Cantoblanco, 28049 Madrid, Spain*

Available online 21 October 2004

Abstract

Fabrication of native Nb oxide barriers and their influence on the tunneling behavior of Nb/Ni planar junctions are investigated. Each junction film electrode was grown by magnetron sputtering technique and two methods were used to obtain the barrier. In the first method, a Nb_xO_y oxide layer was formed at room conditions on top of Nb. In the second one, a saturated water vapor atmosphere is used to obtain the Nb_xO_y layer. Samples prepared on these ways show different tunneling characteristics related with changes in the barrier. Characterization of the barrier was done by low-angle X-ray diffraction, atomic force microscopy and X-ray photoelectron spectroscopy.

© 2004 Elsevier B.V. All rights reserved.

PACS: 73.40.Gk; 75.70.-i

Keywords: Magnetic/superconducting planar junctions; Tunneling; Magnetic thin films

Tunneling-related phenomena are one of the main topics in magnetic devices based on thin films and multilayers. The use of reliable barriers is crucial for spin-polarized effects [1]. Recently, good quality Nb/Ni superlattices have been reported [2]. In this work we have studied the possibility to fabricate planar tunnel junctions using this magnetic/superconducting system.

Planar junctions consisting of superconducting Nb and magnetic Ni have been fabricated by magnetron sputtering keeping an Ar pressure of 1 mTorr during the evaporation at room temperature. These conditions ensure a Nb roughness less than 0.3 nm [3] and superconducting critical temperatures of 8.6 K. To obtain the junction, first, a 100 nm thickness Nb film is deposited on a Si substrate. After this, the film is chemically etched to make the 1 mm width strip of the first electrode. The next step is the tunnel barrier preparation, which has been done following two different methods. In the first one (labeled *dry*

*Corresponding author. Tel.: +34 91 394 4548; fax: +34 91 394 4547.

E-mail address: cynus@fis.ucm.es (E.M. González).

Oxygen), a Nb_xO_y oxide layer was formed at room conditions on top of Nb strip. In the second one (labeled *wet* Oxygen), the Nb_xO_y layer was obtained after the Nb strip was in a saturated water vapor atmosphere. Finally, a mask is used during the evaporation of Ni (60 nm thickness), on top of the Nb electrode with the oxide barrier on top, to produce cross strips of 0.5 mm width. Refinement [4] of low-angle X-ray scan allows us to extract the oxide barrier layer thickness (around 13 Å and 25 Å for *dry* and *wet* methods, respectively).

In order to study the influence of the very different oxidation conditions on the quality of the barrier, both the chemical composition and roughness of the native Nb oxide films were characterized by X-ray photoelectron spectroscopy (XPS) and atomic force microscopy (AFM), respectively. XPS measurements were performed in a PHI spectrometer equipped with a double pass CMA using Mg K_{α} radiation ($h\nu = 1253.6$ eV). On the other hand, the barrier behavior in tunneling configuration was investigated by means of characteristic dynamic resistance (dV/dI) versus bias voltage (V) using a conventional bridge and lock-in amplifier techniques. Measurements were done using a He-range temperature cryostat.

Upon inspection of the XPS spectra, the only presence of the characteristic Nb and O core levels is shown. A detailed line shape analysis of the Nb(3d) spectra has been performed following the indications given in Ref. [5], and using the fitting parameters given in the literature for Nb and their oxide phases [6].

Fig. 1 displays Nb(3d) XPS core level photoemission spectra for the oxidation methods corresponding to (a) *dry* and (b) *wet* processes. Dots represent the raw data, which are superimposed to a solid line result of a fit in terms of several Nb(3d) derived doublets and a secondary electron background subtraction. The analysis of the spectra shape and the decomposition into different components illustrates the nature of the oxide layers formed, and it permits to identify the different oxide phases. This chemical identification has been performed by the assignation of these components to different Nb oxidation states, with characteristic energy shifts with respect to the Nb^0 metal, in good agreement with the

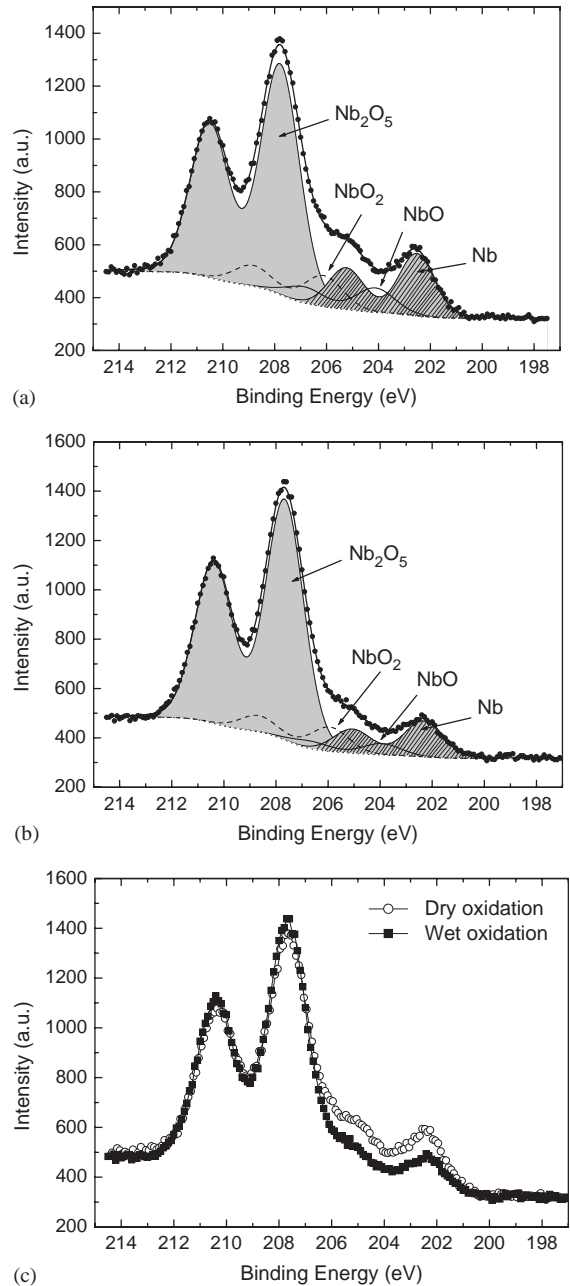


Fig. 1. Nb(3d) XPS core level photoemission spectra for the Nb film oxidation under (a) *dry*, (b) *wet* oxygen exposure, recorded using Mg- K_{α} radiation. Spectra are decomposed into several components, which correspond to bulk-metallic and oxides phases, and background subtraction. (c) Comparison of Nb(3d) spectra for the above oxidation processes to illustrate the higher emission from metallic Nb in the case of *dry* oxidation.

values reported (Nb^{2+} : -1.60 eV, Nb^{4+} : -3.60 eV, and Nb^{5+} : -5.35 eV) [6].

The results obtained reveal the presence of the same oxide phases Nb^{2+} , Nb^{4+} and Nb^{5+} in both films. Likewise, the relative intensity of the different oxidation states indicates that the oxide layer is mainly composed of the dielectric Nb_2O_5 as the outermost layer. On the contrary, metallic suboxide components of lower oxidation phases remain constrained to the Nb–Ni interface. Moreover, a much higher intensity from the component associated to the underneath Nb metal (Nb) is observed for the *dry* method (see Fig. 1(c)). This can be explained in terms of a different growth mode and morphology of the barrier; that is, the barrier could have more pinholes, island or high roughness through which the XPS technique is able to explore and get information of the Nb underneath the thin oxide layer. This different morphology might affect the tunneling properties of the junction somehow. Therefore, in order to elucidate whether any morphological modification had place when the oxide layer is formed under different conditions, AFM measurements were carried out, as shown in Fig. 2. The AFM images evidenced the presence of pinholes in the Nb oxide layers formed, although it can be minimized in the case of *wet* method. In contrast, despite the very close features found in their topography, very

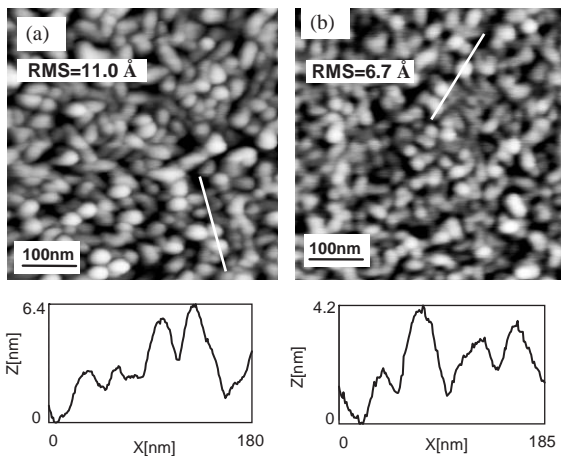


Fig. 2. AFM measurements of Nb oxide barriers formed under (a) *dry*, and (b) *wet* Oxygen method.

significant differences in the roughness values of 11.0 and 6.7 Å are measured for the barriers formed under *dry* and *wet* Oxygen methods, respectively. This result could explain the lower Nb^0 intensity observed in the XPS spectra of the barrier under wet oxidation conditions since this procedure give rise to a more compact and continuous barrier with reduced number of pinholes.

Fig. 3 shows the influence of the barrier prepared following the *dry* Oxygen method on the experimental behavior of dV/dI versus V for a Nb/Ni junction at $T = 1.52$ K. The most surprising features are the reduced value of the Nb superconducting energy half-gap $\Delta = 0.31$ meV, as extracted from the positions of the minima peaks, and the so-called zero bias anomaly; both things indicate a tunneling behavior far from ideal. However, a different characteristic is obtained when the tunnel barrier is fabricated following the *wet* Oxygen process (see Fig. 4). In this case, a value of $\Delta = 1.4$ meV is extracted in agreement with the Nb bulk energy gap. The big difference observed in the gap value could be related with the barrier quality. In fact, as revealed by XPS and

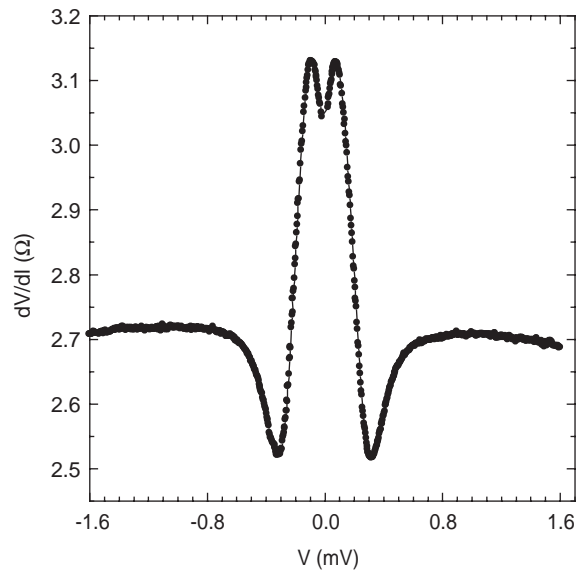


Fig. 3. Differential resistance (dV/dI) as a function of bias voltage (V) of a planar Nb/barrier(Nb_xO_y)/Ni junction at $T = 1.52$ K with barrier prepared following *dry* Oxygen method (see text for details).

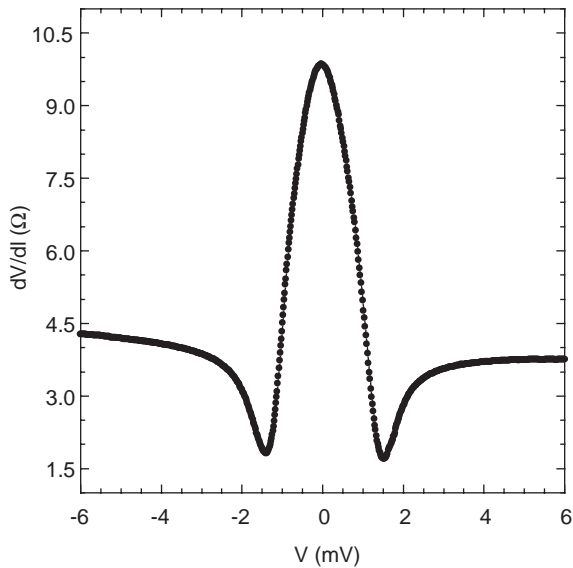


Fig. 4. Differential resistance (dV/dI) versus bias voltage (V) of a planar Nb/barrier(Nb_xO_y)/Ni junction at $T = 1.52$ K with barrier prepared following *wet* Oxygen method (see text for details).

AFM, the higher number of pinholes and roughness of *dry* Oxygen barrier makes the influence of the magnetic Ni electrode to be stronger than in the case of *wet* Oxygen barrier, thus reducing the superconducting order parameter in a Nb sheet close to the junction interface. However, both characteristics ($dV/dI-V$) are similar in the sense that they do not exhibit a well-defined superconducting gap with very high value of the resistance for voltages $eV < \Delta$, although higher

values are reached for the *wet* case. Therefore, junctions with better signature of tunneling are obtained for this last case although the corresponding dV/dI curve is still far from ideal. The presence of different oxidation states could affect not only the tunneling process but also the polarization distribution via scattering process.

Acknowledgements

Work supported by Spanish C.I.C.Y.T. (MAT2002-04543) and ESF Vortex Program. E. M. González acknowledges Ministerio de Ciencia y Tecnología for a Ramón y Cajal contract. R. Escudero (on leave from IMM-Universidad Nacional Autónoma de México) thanks Universidad Complutense and Ministerio de Educación, Cultura y Deporte for a sabbatical professorship.

References

- [1] J.M. De Teresa, A. Barthélémy, A. Fert, J.P. Contour, F. Montaigne, P. Seneor, *Science* 286 (1999) 507.
- [2] E. Navarro, J.E. Villegas, J.L. Vicent, *J. Magn. Magn. Mater.* 240 (2002) 586.
- [3] J.E. Villegas, E. Navarro, D. Jaque, E.M. González, J.I. Martín, J.L. Vicent, *Physica C* 369 (2002) 213.
- [4] E.E. Fullerton, I.K. Schuller, H. Vanderstraeten, Y. Bruynseraede, *Phys. Rev. B* 45 (1992) 9292.
- [5] J.J. Joyce, M. Del Giudice, J.H. Weaver, *J. Electron. Spectrosc. Relat. Phenom.* 49 (1989) 31.
- [6] A. Darlinski, J. Halbritter, *Surf. Interface Anal.* 10 (1987) 223.